

Structure and morphology of phenylsilanes polymer films synthesized by the plasma polymerization method

H. NAGAI, Y. NAKATA, M. SUZUKI, T. OKUTANI

Hokkaido National Industrial Research Institute 2-17-2-1, Tsukisamu-higashi, Toyohira-ku, Sapporo 062, Japan

E-mail: nagai@hniri.go.jp

Phenylsilanes were deposited by r.f. glow discharge to investigate the relationship between the synthesis conditions (r.f. power, synthesis time and monomer) and the structure and morphology of plasma-polymerized films. The film deposited at 2.0 W consisted of polycarbosilane-like main chains and side chains corresponding to the monomer structure. The film deposited at higher r.f. power consisted of a polycarbosilane-like main chain with more cross-links and less aromatic groups. The films synthesized at 2.0 W from phenylsilane had many submicrometre sized particles on the surface, but the films synthesized from phenylsilanes with methyl groups had few particles and smooth surfaces. The films deposited at higher r.f. power had many particles on their surfaces. The infrared spectra of methylphenylsilane polymer films were independent of the synthesis time, but film surface morphology changed from a smooth surface into a granular surface with an increase in the synthesis time. © 1998 Chapman & Hall

1. Introduction

Organosilicon polymers are expected to be new functional materials [1–3]. Polysiloxanes, a kind of organosilicon polymer, are already produced industrially and applied to many fields because of their heat resistivity, weather resistivity and chemical stability [4]. Many organosilicon polymers, except polysiloxane, are still produced on a laboratory scale, but many researchers are currently investigating new and improved methods of synthesis and characterizations of these polymers. The starting materials of carbon-based polymers with functional groups for polymerization, such as double bonds and triple bonds, etc., can be easily synthesized. However, the starting materials of organosilicon polymers are mainly chlorosilanes and the methods of synthesis are limited compared with those of carbon-based polymers [5–8]. The plasma polymerization method is known as the method by which polymerized materials are easily obtained, even if the monomer does not have functional groups for polymerization [9]. Therefore, polymers are synthesized from any chemical compound using the plasma polymerization method, and are used in various ways, such as films for separation, protection and insulation [9]. In many cases, the structure of polymer films synthesized by the plasma polymerization method is independent of the monomer structure. Because plasma energy is too strong for polymerization, the competitive reactions of deposition and ablation of the polymer films which occur in plasma polymerization (CAP mechanism) [10] causes the functional group in polymer films to be destroyed.

In order to control the organic polymer structure, pulse electric discharge [11], mesh screen [12], and low-power plasma polymerization [13–15] were investigated. In this study, phenylsilane monomers were used and the relationship between monomers and the structure of polymerized film under low-power plasma was investigated.

2. Experimental procedure

2.1. Chemical reagents and substrate

Phenylsilane ($C_6H_5-SiH_3$, PS), methylphenylsilane ($C_6H_5-SiH_2CH_3$, MPS), dimethylphenylsilane ($C_6H_5-SiH(CH_3)_2$, DMPS) and trimethylphenylsilane ($C_6H_5Si(CH_3)_3$, TMPS) (Shin-Etsu Chemical Co. Ltd) were used as monomers. These monomers were frozen by liquid nitrogen and degassed before the experiments. Silicon wafers (10 mm × 10 mm × 0.3 mm, ultrasonically washed in acetone) were used as a substrate.

2.2. Experimental procedure

The polymer films were deposited on the substrate in an inductively coupled plasma apparatus (13.56 MHz; electric discharge coil, 7 turns; reactor inner diameter, 22 mm) as shown in Fig. 1.

The synthesis conditions of the polymer films were as follows. The substrates were placed in the reactor so that the deposition rate of the films was at a maximum. The system was evacuated to 0.4 Pa and then argon gas (purity >99.9995%) was introduced into

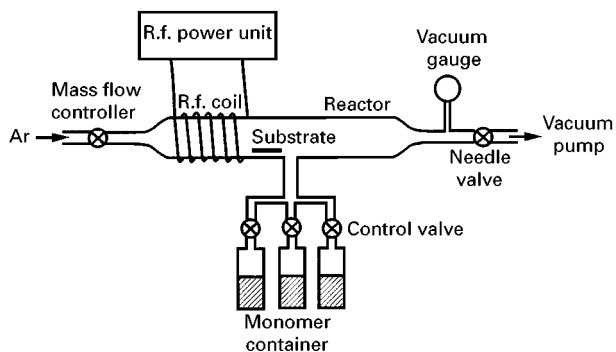


Figure 1 Schematic diagram of the reactor system.

the reactor at a flow rate of $1.0 \times 10^{-6} \text{ m}^3 \text{ min}^{-1}$ until the pressure in the reactor was 10.0 Pa. The argon plasma was generated at 50 W for 1 h to eliminate water and contamination on the substrate surface and on the inner wall of the reactor. Then, the monomer gas was introduced into the reactor until the total gas pressure reached 16.0 Pa. Then it was polymerized at 2.0–20.0 W for 0.5–3 h. After synthesis of the polymer films, the reactor was evacuated to 0.4 Pa. The reactor was pressurized again to 10 Pa using argon gas. The polymerized films were left for 1 h in the argon gas and removed from the reactor.

2.3. Characterization of polymer films

The infrared (IR) spectra of the polymer films were measured by a Perkin–Elmer 1600 Fourier transform–infrared (FT–IR) spectrometer. The Raman scattering measurements were performed using a Spex ramalog-10 system. The X-ray photoelectron spectroscopy (XPS) spectra were recorded on a Kratos XSAM-800 photoelectron spectrometer employing MgK_α radiation, and the binding energy scale was calibrated by measuring the Au $4f_{7/2}$ core level (binding energy $E_B = 84.0 \text{ eV}$). The ultraviolet (UV) reflection spectra were measured by a Shimadzu UV-1200 spectrometer. The surface morphology and the thickness of the polymer films were observed and measured using a Jeol JXA-8600 X-ray microanalyser.

3. Results and discussion

3.1. Effect of r.f. power on the structure of MPS polymer films

MPS plasma-polymerized films were synthesized at various r.f. powers for 1 h. The IR spectra of the polymer films are shown in Fig. 2 and the assignments of IR absorption bands are listed in Table I. The polymer films synthesized at any r.f. power showed absorption during the stretching of aromatic C–H bonds (Band A), aliphatic C–H bonds (Band B), and Si–H bonds (Band C). Absorption during the deformation of Si– CH_3 bonds (Band G) and characteristic absorption of benzene bands (Band D) and monosilylbenzene bands (Band F) was also observed. This is similar to the IR spectrum of a MPS monomer. The broad absorption bands of Si–C bonds and the weak

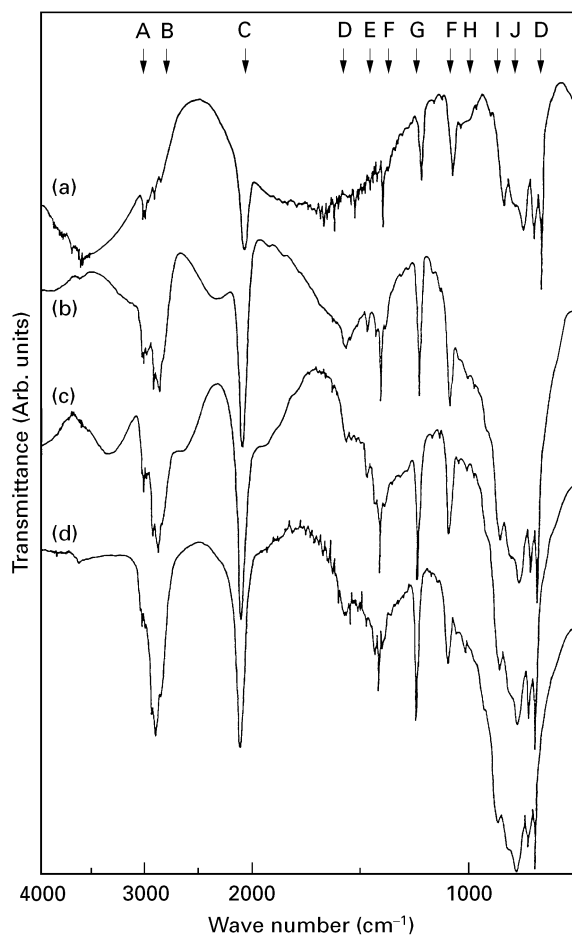


Figure 2 FT–IR spectra of MPS plasma polymerized films prepared at different r.f. power. Synthesis conditions: time 1 h; r.f. power (a) 2.0 W, (b) 5.0 W, (c) 10.0 W, (d) 20.0 W.

TABLE I Characterization of IR bands

Band (Figures)	Assignments	Wave number (cm^{-1})
A	C–H stretching in aromatic ring	3077–3006
B	C–H stretching CH_2 , CH_3	2930–2852
C	Si–H stretching in Si– H_x	2156–2108
D	Characteristic bands of substituted benzene	1601–1575 1495–1483 1117–1074 756–733 700–698
E	C–H bending	1460–1451
F	Characteristic bands of monosilylbenzene	1429–1427 1117–1105
G	– CH_3 deformation in Si– $(\text{CH}_3)_n$	1270–1240
H	(1) – CH_2 – wagging in Si– $(\text{CH}_2)_2$ –Si, Si– CH_2 –Si (2) Si–O stretching in Si–O–Si, Si–OR (3) C–C stretching	1067–1020
I	(1) Si–H bending in Si– H_x (2) Si–C stretching	922–791
J	– CH_3 rocking in Si– $(\text{CH}_3)_n$	857–804

absorption bands of Si–O bonds were observed in all films. The peak height ratio of Band A to Band B increased with decreasing r.f. power. This phenomenon is presumed to suppress the phenyl ring-opening

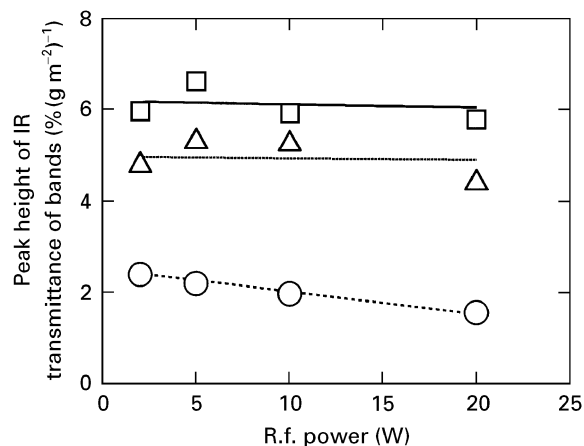


Figure 3 Effect of r.f. power on peak height of IR transmittance of various bands of MPS plasma polymerized films. (○) C–H stretching in aromatic ring (Band A), (□) Si–H stretching in Si–H_x (Band C), (△) –CH₃ deformation in Si–(CH₃)_n (Band G).

reaction at low r.f. power. The peak heights of Bands A, C and G measured from each IR spectrum are shown in Fig. 3. Because of the different film weights, each peak height was converted into per 1.0 g m⁻² of polymer films. The peak heights of Si–H and Si–CH₃ bonds slightly increased, and those of aromatic C–H bonds increased with decreasing r.f. power. This result showed that the amount of aromatic group in the polymer film increased with decreasing r.f. power. Our result was in agreement with those of Inagaki *et al.* [14] and Nakamura *et al.* [15].

Table II shows the binding energies, linewidths and elemental ratios (C/Si, O/Si) of the XPS spectra for these polymerized films. Those of chemically synthesized polymethylphenylsilane (PMPS) and polymethylcarbosilane (PMCS) (Shin-Etsu Chemical Co. Ltd.) are also shown in Table II. The binding energies of Si 2p and C 1s for these plasma-polymerized films were 99.9–100.1 eV and 283.9–284.0 eV, respectively. Gray *et al.* [16] and Inagaki *et al.* [14] reported the assignment of Si 2p binding energies for organosilicon compounds. The binding energies of Si 2p for the plasma-polymerized films showed that a large amount of silicon atoms in the polymer films were bonded by two or more carbon atoms. Fig. 4 shows the C 1s XPS spectra of PMPS, PMCS and MPS plasma-polymerized films. The C 1s spectrum of PMPS was a

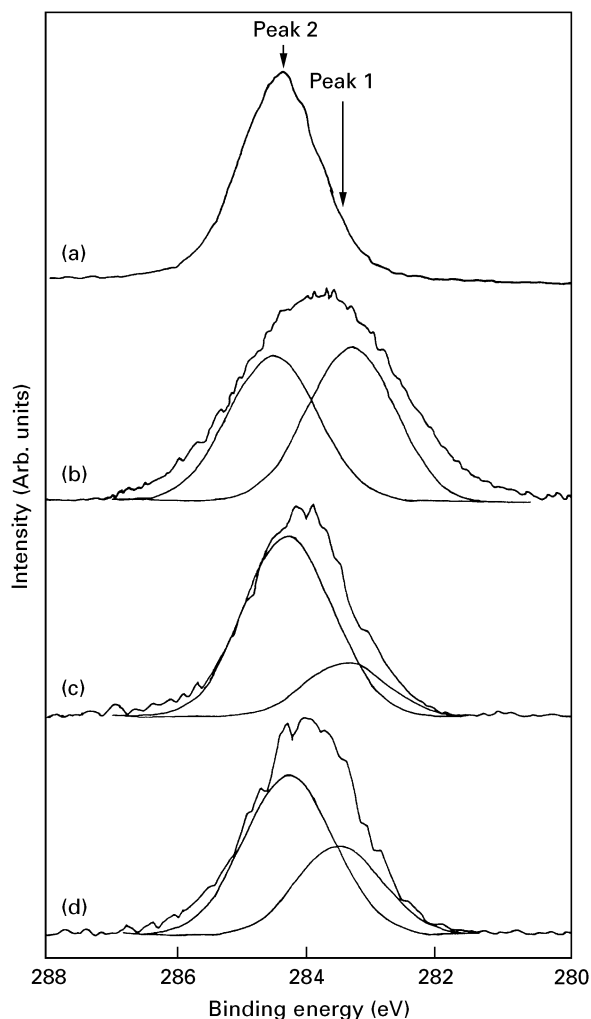


Figure 4 C 1s XPS spectra of MPS plasma polymerized films. (a) PMPS, (b) PMCS, (c) MPS plasma polymer film (2.0 W, 1.0 h), (d) MPS plasma polymer film (20.0 W, 1.0 h).

single peak, while that of PMCS was separated into two peaks. It was assumed that the peak of 283.4 eV (Peak 1) was based on the carbon of the polycarbosilane main chain (–Si–CH₂–Si–) and the peak of 284.6 eV (Peak 2) was based on the carbon of the methyl group (–Si(CH₃)–) or the phenyl group (–Si(C₆H₅)–). The C 1s peaks of the plasma-polymerized films could also be separated into two peaks. The area ratio of Peak 1 to Peak 2 increased with

TABLE II Binding energies, linewidths and element ratios of the XPS spectra of the MPS plasma polymerized films prepared at different r.f. power

Monomer	R.f. power (W)	Si 2p		C 1s		Peak separation			Element ratio (at %)	
		EB (eV)	FWHM (eV)	EB (eV)	FWHM (eV)	EB (eV)		Area ratio (Peak 1/Peak 2)	C/Si	O/Si
						Peak 1	Peak 2			
MPS	2	100.0	2.3	283.9	1.7	283.3	284.2	0.27	7.1	0.7
	5	100.1	2.3	284.0	1.8	283.4	284.3	0.33	8.1	0.9
	10	99.9	2.1	283.9	1.9	283.2	284.2	0.40	7.9	0.7
	20	100.0	2.1	283.9	1.9	283.5	284.3	0.54	8.3	0.8
PMPS		99.7	1.4	284.4	1.4		284.4	0	7.1	0.1
PMCS		100.5	2.3	283.9	2.7	283.4	284.6	1.04	3.5	0.3

increasing r.f. power. This result showed that cross-link structures in plasma-polymerized films developed with increasing r.f. power because the amount of carbon atoms surrounded by several silicon atoms increased with increasing r.f. power. The C/Si ratio of the film synthesized at 2.0 W was 7.1, similar to that of the monomer (C/Si = 7), and the ratio of C/Si in the polymer films also increased with r.f. power. Nakamura *et al.* reported that the concentration of $C_6H_6^+$ and its fragmented ionic species (CH_3^+ , $C_2H_2^+$, etc.) increased with increasing r.f. power [15]. The increase of the C/Si ratio for an increase in r.f. power may be caused by the contribution of these ionic species to the polymerization reaction.

Fig. 5 shows the UV spectra of the plasma-polymerized films. With increasing r.f. power, the absorption band spread from 370 nm to around 550 nm. The UV absorption caused by $\pi-\pi^*$ transition in the individual phenyl side chain appears around 280 nm [17], but it is difficult to explain the wavelength absorption longer than 300 nm by $\pi-\pi^*$ transition. It is well known that polysilanes have an intense absorption in the near UV region, owing to the σ -delocalization in the Si-Si chain [1]. The monomers and polymers with Si-Si bonds showed the Raman band in the region from 330–470 cm^{-1} [18–20]. However, the MPS plasma-polymerized films did not contain Si-Si bonds, because they did not show any Raman band in the region from 100–500 cm^{-1} . Therefore, this longer wavelength UV absorption is not considered to be due to the σ -delocalization in the Si-Si chain. Nakamura *et al.* [15] reported that the optical band gap of MPS plasma-polymerized films decreased with increasing r.f. power, that is, the absorption band spread towards longer wavelength with increasing r.f. power (for example, the absorption band of the films synthesized at 2.0 W spread towards about 470 nm, and that of 10.0 W spread towards about 690 nm), and they attributed it to amorphous silicon carbide-like structure in the film. The structure of our plasma-polymerized film at high r.f. power was considered to be very similar to the structure of amorphous silicon carbide [21], because the cross-link structures in the plasma-polymerized films developed with increasing r.f. power [22, 23]. The longer wavelength UV absorption might be due to the formation of amorphous silicon carbide-like structure caused by the development of Si-C cross-linkage.

The structure model of MPS plasma-polymerized films at low and high r.f. power plasma is illustrated in Fig. 6. At low-power plasma, the polymer film consisted of a polycarbosilane main chain and phenyl rings and methyl groups as side chains with less cross-link structures. At high-power plasma, the polymer film contained many cross-linkages and less phenyl rings as side chains.

Fig. 7 shows scanning electron micrographs of the MPS plasma-polymerized films. The film synthesized at 2.0 W had a smooth surface, but for films synthesized at higher r.f. power, 0.2–1.0 μm particles were observed on the films synthesized at higher r.f. power.

Fig. 8 shows the dependence of the deposition rate and the film density on r.f. power. The deposition rate

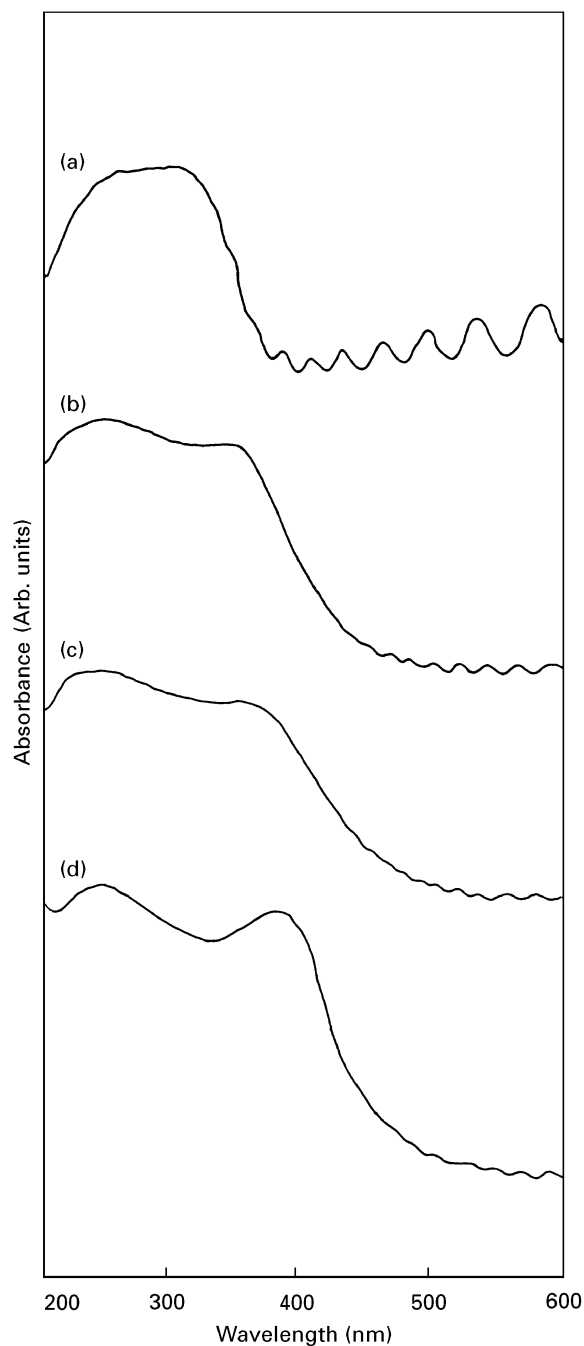
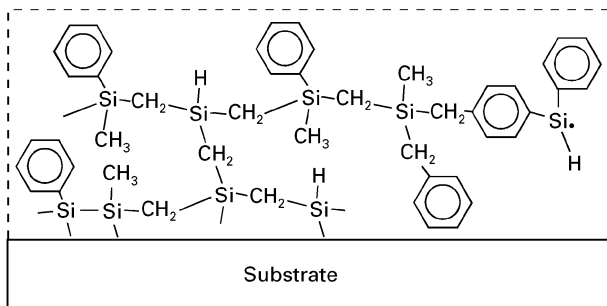


Figure 5 UV spectra of plasma polymerized MPS films prepared at different r.f. power. Synthesis conditions: time 1 h; r.f. power (a) 2.0 W, (b) 5.0 W, (c) 10.0 W, (d) 20.0 W.

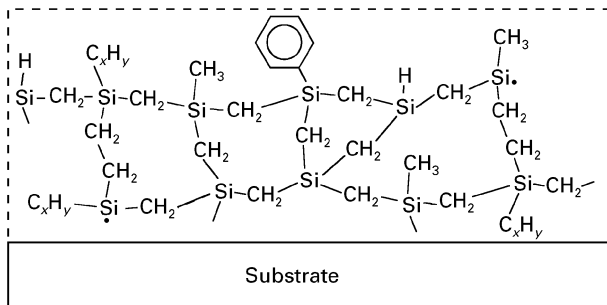
increased as r.f. power increased, but the film densities were nearly the same. Kobayashi *et al.* reported that a granular surface was easily observed with an increasing deposition rate [24]. It was assumed that the granular surface of Fig. 7 was formed because of a high deposition rate.

3.2. Effect of synthesis time on the structure of MPS polymer films

The MPS plasma-polymerized films were synthesized at 2.0 W for various polymerization times. The IR spectra of the films showed the same pattern, while all peak intensities increased with polymerization time. The UV spectra of the polymerized films gradually spread towards longer wavelengths with increasing



(a)



(b)

Figure 6 Model structures of MPS plasma polymer films.

time. These results show that the side chain structures in the polymer films are similar and that the main chain cross-link bonds increased with increasing time.

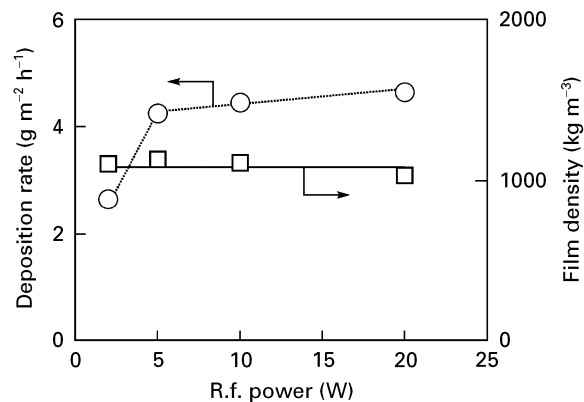


Figure 8 Deposition rate (○) and film density (□) of MPS plasma polymerized film.

Fig. 9 shows scanning electron micrographs of the polymer films at various polymerization times. The film that was synthesized for 1 h had a smooth surface. As synthesis time increased, 0.2–1.0 μm particles were observed on the film surfaces and some particles grew and combined into large lumps, like a cauliflower. With increasing time, the deposition rate (Fig. 10) gradually decreased, but the film density gradually increased. Generation and growth of particles on the deposited film might be due to the activation of the polymer film surface by ablation. The increase in the film density was assumed to be caused by the increase of cross-link bonds in the deposited film.

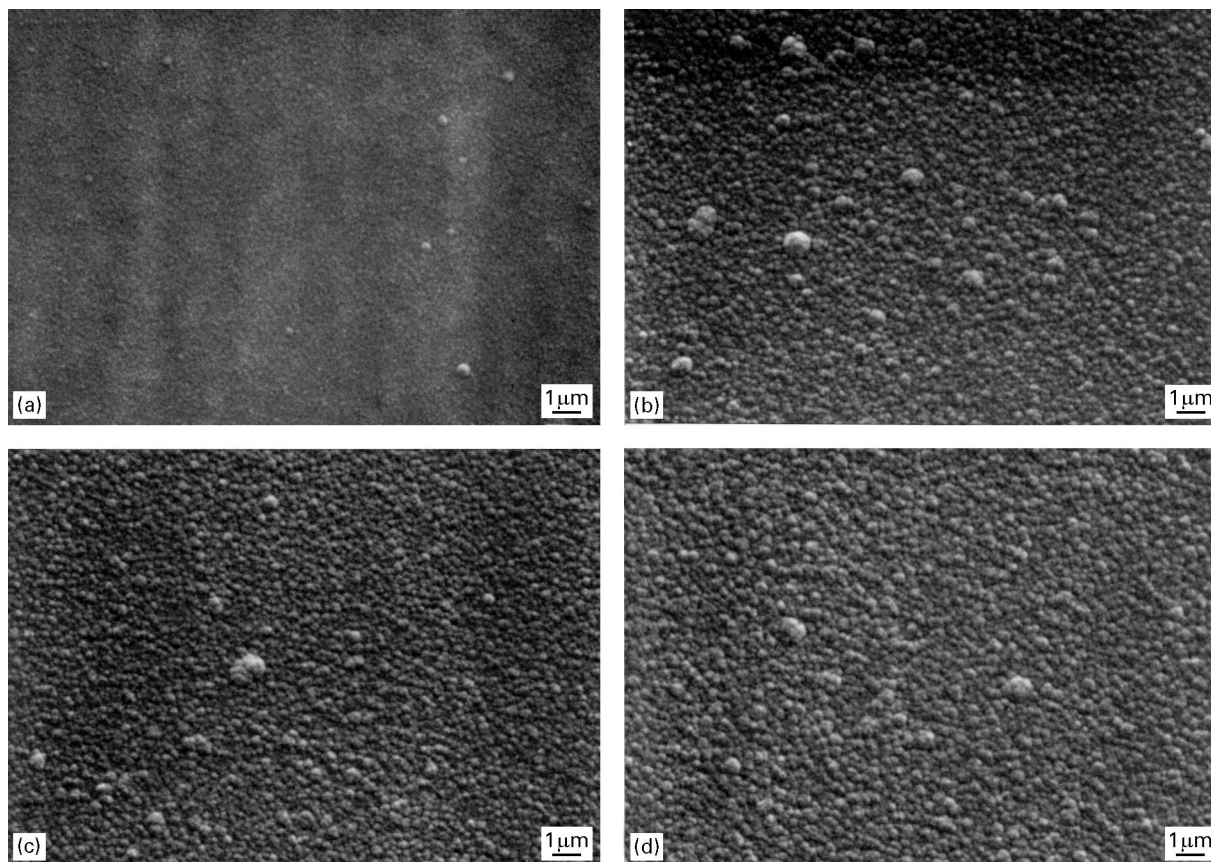


Figure 7 Scanning electron micrographs of MPS plasma polymerized films prepared at different r.f. power. Synthesis conditions: time 1 h; r.f. power (a) 2.0 W, (b) 5.0 W, (c) 10.0 W, (d) 20.0 W.

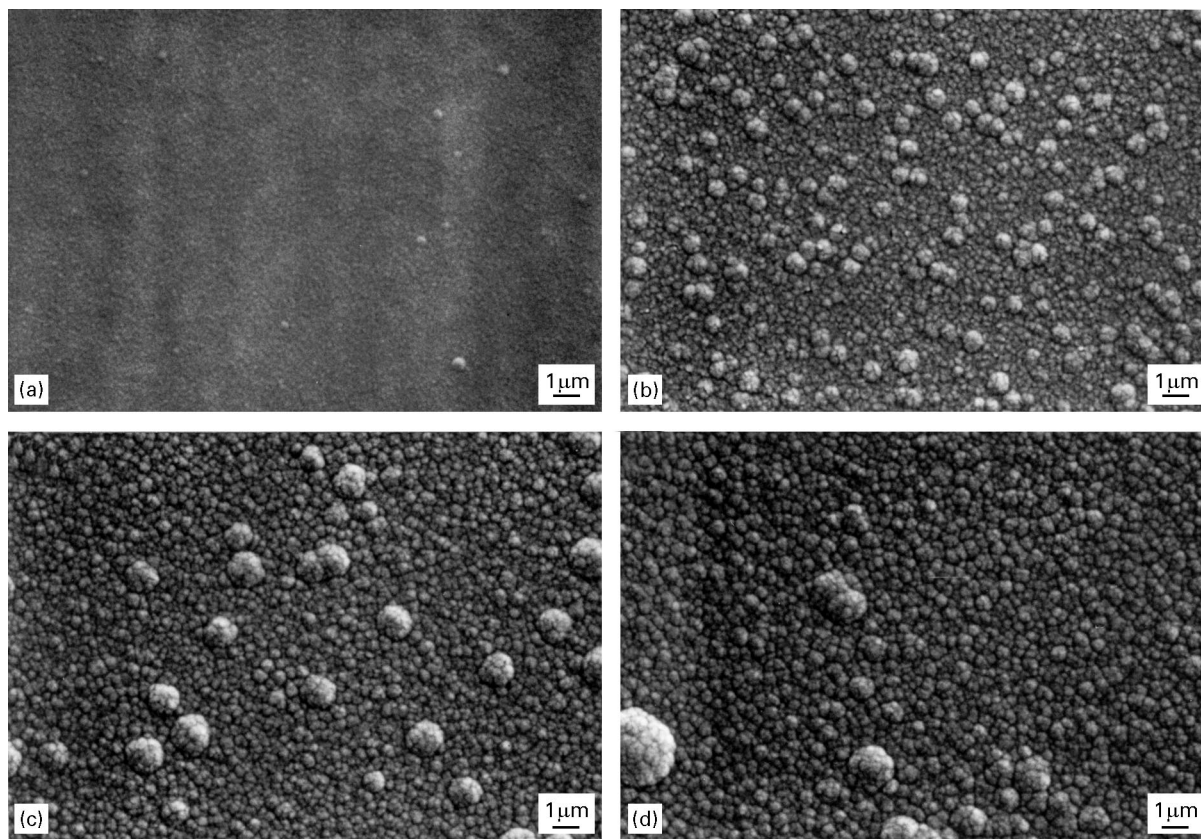


Figure 9 Scanning electron micrographs of MPS plasma polymerized films prepared at different synthesis time. Synthesis conditions: r.f. power 2.0 W, time (a) 1.0 h, (b) 1.5 h, (c) 2.0 h, (d) 3.0 h.

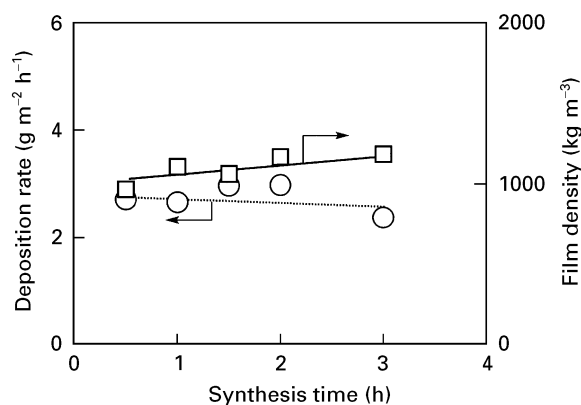


Figure 10 Deposition rate (○) and film density (□) of MPS plasma polymerized film.

3.3. Effect of monomer on the structure of the plasma-polymerized films

Fig. 11 shows the IR spectra of the films synthesized at 2.0 W for 1 h from various phenylsilane monomers. The plasma-polymerized films showed some characteristic absorption bands similar to their corresponding monomers, such as phenyl rings, Si–H bonds, Si–CH₃ bonds, etc. The PS plasma-polymerized films had weak absorption based on the Si–CH₃ bonds. The TMPS polymer film had weak absorption based on the Si–H bonds. The absorption bands based on aliphatic C–H bonds (Bands B, G, J) increased, but those with Si–H bonds (Band C) decreased as the

number of methyl groups in the monomer increased. The peak heights of aromatic C–H bonds (Band A), Si–H bonds (Band C) and Si–CH₃ bonds (Band G) are shown in Fig. 12. The peak height of Band G increased linearly as the number of methyl groups in the monomer increased, but that of Band C decreased linearly with increasing methyl groups. The peak heights of Band A were nearly the same. Therefore, the low-power plasma-polymerized films had similar side chains to the monomers and the structure of the plasma-polymerized films reflected that of the monomer structures. The structure of the low-power plasma-polymerized film could be controlled by changing monomers.

Binding energies, linewidths and elemental ratios (C/Si, O/Si) of the XPS spectra of these polymerized films are listed in Table III. The binding energies of Si 2p and C 1s of these polymer films were nearly the same, but the FWHM values of Si 2p spectra decreased on using a DMPS and a TMPS monomer, due presumably to a decrease in the oxygen component (Si–(O–C)_{2 or 3}, Si–O). The C 1s spectra of the polymer films were also separated into two peaks, Peaks 1 and 2, like Fig. 4. The peak ratio of Peaks 1 and 2 tended to decrease with an increase in the number of monomer methyl groups. The C/Si ratios of the polymer film surface were similar to that of the monomer.

Fig. 13 shows the UV spectra of the plasma-polymerized films prepared from various monomers. The absorption band spread from 350–450 nm depending on the number of methyl groups in the monomer. As

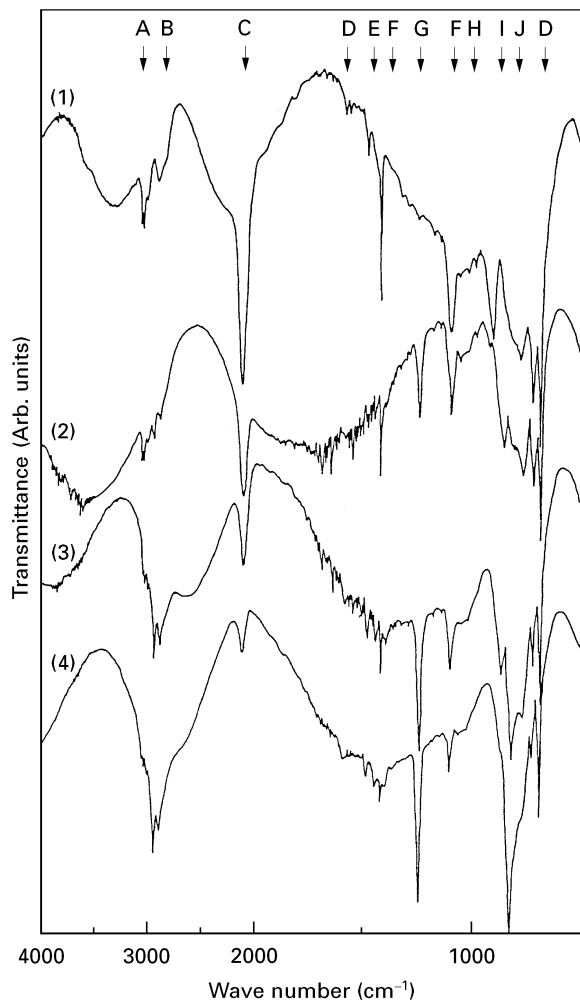


Figure 11 FT-IR spectra of plasma polymerized films prepared from phenylsilanes monomer. Synthesis conditions: r.f. power 2.0 W, time 1.0 h, monomer (1) PS, (2) MPS, (3) DMPS, (4) TMPS.

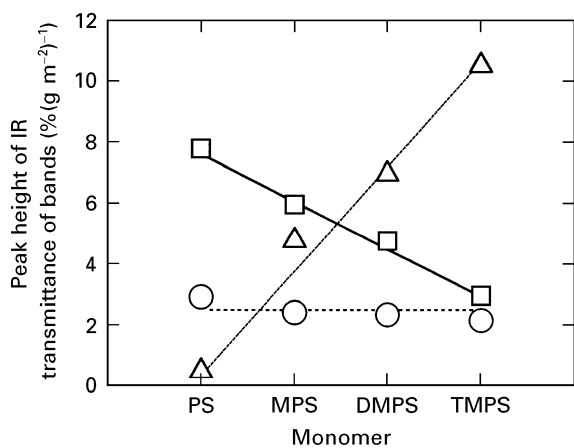


Figure 12 Effect of monomer on peak height of i.r. transmittance of various bands of plasma polymerized films prepared at 2.0 W. (○) C-H stretching in aromatic ring (Band A), (□) Si-H stretching in Si-H_x (Band C), (△) -CH₃ deformation in Si-(CH₃)_n (Band G).

Si-H bonds are weaker than C-H bonds, Si-H bonds were easily broken by plasma and contributed to the polymerization. The reaction site increased and the cross-linkages increased with the number of Si-H bonds in monomer. Therefore, the cross-linked

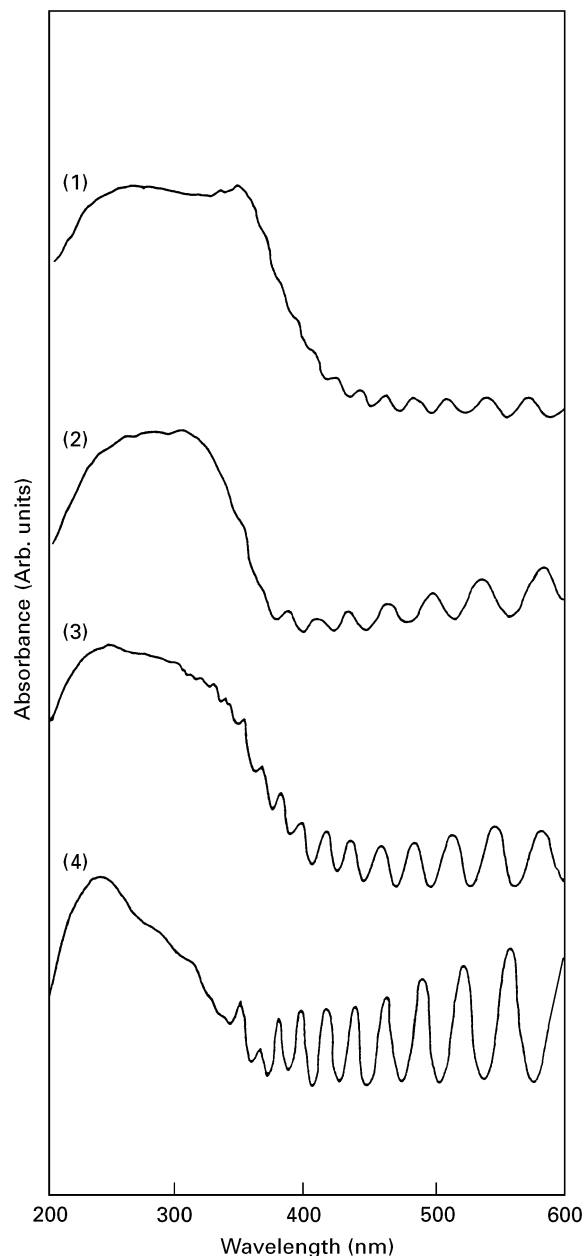


Figure 13 UV spectra of plasma polymerized films prepared from phenylsilanes monomer. Synthesis conditions: r.f. power 2.0 W, time 1 h, monomer (1) PS, (2) MPS, (3) DMPS, (4) TMPS.

structure of Si-C would develop in the order of PS > MPS > DMPS > TMPS and the UV absorption band spread towards longer wavelengths in the same order. These polymer films did not show any Raman band in the region from 100-500 cm⁻¹. This longer wavelength UV absorption might be due to the formation of amorphous silicon carbide-like structure caused by Si-C cross-linkage.

Fig. 14 shows scanning electron micrographs of the polymer films. The surface of the film synthesized from PS showed many 0.4-0.8 μm particles on the surface, but those of the films synthesized from the monomer including methyl groups had smoother surfaces. As shown in Fig. 15, the deposition rate and film density were nearly the same, except for the density of the polymer film synthesized from PS. This result shows that PS is easy to polymerize, and it was considered that the plasma-polymerized film prepared from PS

TABLE III Binding energies, linewidths and element ratios of the XPS spectra of the plasma polymerized films prepared from phenylsilanes monomer

Monomer	R.f. power (W)	Si 2p		C 1s		Peak separation			Element ratio (at %)	
		EB (eV)	FWHM (eV)	EB (eV)	FWHM (eV)	EB (eV)		Area ratio (Peak 1/Peak 2)	C/Si	O/Si
						Peak 1	Peak 2			
PS		100.2	2.3	284.2	1.8	283.9	284.6	0.53	6.4	0.8
MPS	2.0	100.0	2.3	283.9	1.7	283.3	284.2	0.27	7.1	0.7
DMPS		100.1	1.9	284.2	1.9	283.4	284.4	0.29	8.3	0.5
TMPS		100.0	1.9	284.2	1.8	283.5	284.3	0.20	8.7	0.5
PMPS		99.7	1.4	284.4	1.4		284.4	0	7.1	0.1
PMCS		100.5	2.3	283.9	2.7	283.4	284.6	1.04	3.5	0.3

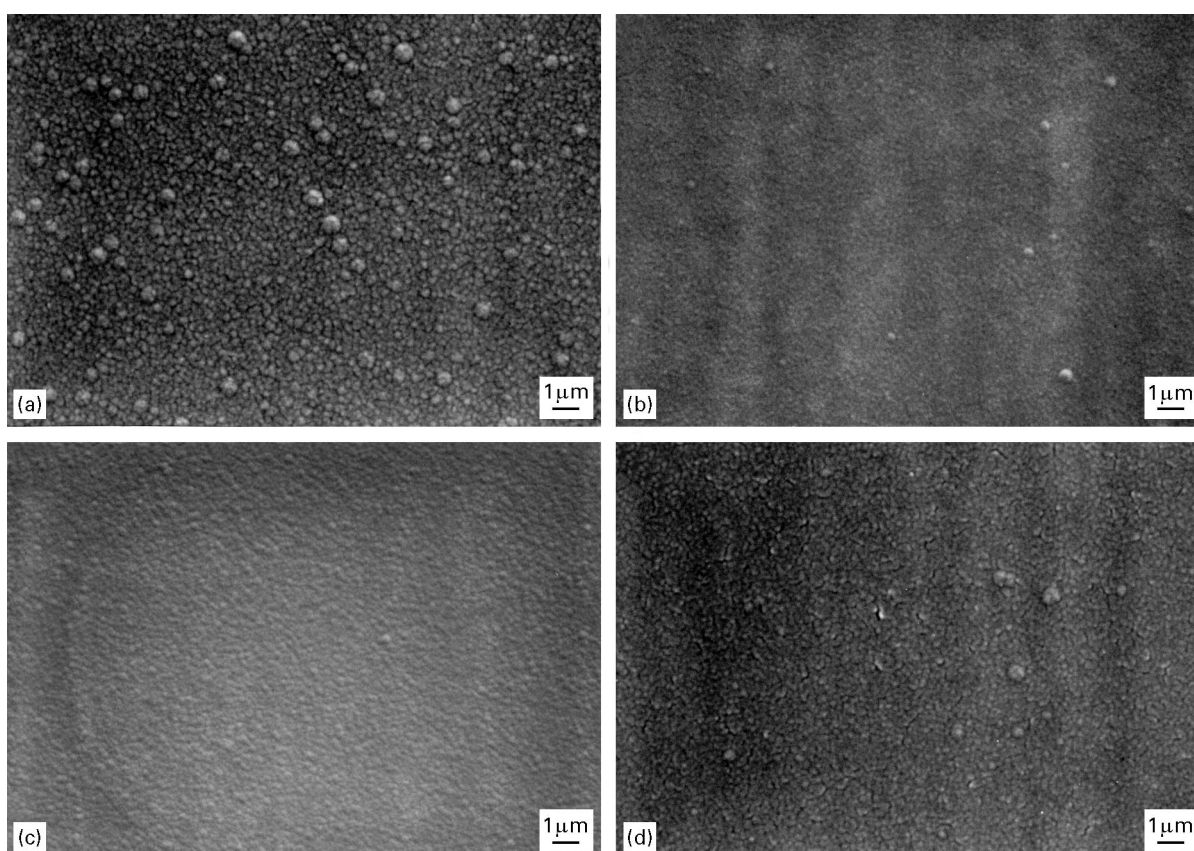


Figure 14 Scanning electron micrographs of plasma polymerized films prepared from phenylsilanes monomer. Synthesis conditions: r.f. power 2.0 W, time 1 h, monomer (1) PS, (2) MPS, (3) DMPS, (4) TMPS.

had more cross-link structures than those prepared from other monomers. The formation of particles on the polymer film surface might be due to an increase of the monomer polymerization rate.

4. Conclusions

1. The MPS plasma-polymerized films consisted of a polycarbosilane main chain with fewer phenyl rings as side chains and more cross-linkages with increasing r.f. power. The UV absorption band spread towards longer wavelength with increasing r.f. power. As r.f.

power increased, many particles were deposited on the surface.

2. The IR spectra of MPS plasma-polymerized films at 2.0 W were independent of the polymerization time, but the UV spectra gradually spread towards longer wavelength with increasing time. As synthesis time increased, many particles were deposited on the surface of the film and some particles grew and combined into larger lumps.

3. The structure of the films synthesized at 2.0 W depends on the monomer structure. The amount of Si-H bonds in the films decreased and that of Si-CH₃ bonds increased with an increase in the number of

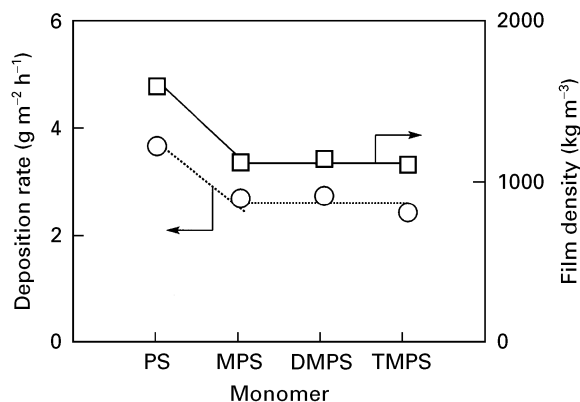


Figure 15 Deposition rate (○) and film density (□) of plasma polymerized film.

monomer methyl groups. As the number of methyl groups decreased, cross-link structures in the plasma-polymerized film were developed and the UV spectra tended to spread towards longer wavelengths. The polymer films synthesized from a monomer with methyl groups showed smoother surfaces than that synthesized from a PS monomer.

Acknowledgement

The authors thank Mr O. Nishimura for the XPS measurements.

References

1. R. D. MILLER and J. MICHL, *Chem. Rev.* **89** (1989) 1359.
2. Z. F. ZHANG, F. BABONNEAU, R. M. LAINE, Y. MU, J. F. HARROD and J. A. RAHN, *J. Amer. Ceram. Soc.* **74** (1991) 670.
3. S. YAJIMA, Y. HASEGAWA, K. OKAMURA and T. MATSUZAWA, *Nature* **273** (1978) 525.

4. A. L. SMITH, "The Analytical Chemistry of Silicones" (Wiley Interscience, New York, 1991).
5. M. ISHIKAWA, *Pure Appl. Chem.* **50** (1978) 11.
6. R. WEST, L. D. DAVID, K. L. STEARLY, K. S. V. SRINIVASIN and H. YU, *J. Amer. Chem. Soc.* **103** (1981) 7352.
7. H. MATSUMOTO, H. MIYAMOTO, N. KOJIMA and Y. NAGAI, *J. Chem. Soc. Chem. Commun.* (1987) 1316.
8. K. SAKAMOTO, K. OBATA, H. HIRATA, M. NAKAJIMA and H. SAKURAI, *J. Amer. Chem. Soc.* **111** (1989) 7641.
9. H. BIEDERMAN and Y. OSADA, "Plasma Polymerization Processes" (Elsevier, Amsterdam, 1992).
10. H. YASUDA, *Koubunshi* **26** (1977) 783.
11. H. YASUDA and T. HSU, *J. Polym. Sci. Polym. Chem. Ed.* **15** (1977) 81.
12. P. D. BUZZARD, D. S. SOONG and A. T. BELL, *J. Appl. Polym. Sci.* **27** (1982) 3965.
13. I. HALLER, *J. Electrochem. Soc.* **129**(1) (1982) 180.
14. N. INAGAKI and H. HIRAO, *J. Polym. Sci. Polym. Chem. Ed.* **24** (1986) 595.
15. T. NAKAMURA, V. A. SINIGERSKY, T. HIRANO, K. FUEKI and H. KOINUMA, *Macromol. Chem.* **189** (1988) 1315.
16. R. C. GRAY, J. C. CARVER and D. M. HERCULES, *J. Electron Spectrosc. Relat. Phenom.* **8** (1976) 343.
17. K. TAKEDA, H. TERAMAE and N. MATSUMOTO, *J. Amer. Chem. Soc.* **108** (1986) 8186.
18. C. C. CERATO, J. L. LAUER and H. C. BEACHELL, *J. Chem. Phys.* **22** (1954) 1.
19. G. W. BETHKE and M. K. WILSON, *ibid.* **26** (1957) 1107.
20. H. LI, I. S. BUTLER and J. F. HARROD, *Appl. Spectrosc.* **47** (1993) 1571.
21. M. M. RAHMAN, C. Y.-W. YANG and G. L. HARRIS, "Springer Proceedings in Physics 43, Amorphous and Crystalline Silicon Carbide II" (Springer, Berlin, 1989).
22. K. NSAKAJIMA, A. T. BELL, M. SHEN and M. MILLARD, *J. Appl. Polym. Sci.* **23** (1979) 2627.
23. D. F. O'KANE and D. W. RICE, *J. Macromol. Sci. Chem.* **A10** (1976) 567.
24. H. KOBAYASHI, M. SHEN and A. T. BELL, *J. Macromol. Sci.* **8** (1974) 373.

Received 23 July 1996
and accepted 22 August 1997